Possible High-Temperature Superconductivity Driven by Perpendicular Electric Field in the La$_3$Ni$_2$O$_7$ Single-Bilayer Film at Ambient Pressure

Zhi-Yan Shao,[1, *] Jia-Heng Ji,[1, *] Congjun Wu,[2, 3, 4, 5] Dao-Xin Yao,[6] and Fan Yang[1, †]

[1]*School of Physics, Beijing Institute of Technology, Beijing 100081, China*
[2]*New Cornerstone Science Laboratory, Department of Physics,*
School of Science, Westlake University, Hangzhou 310024, Zhejiang, China
[3]*Institute for Theoretical Sciences, Westlake University, Hangzhou 310024, Zhejiang, China*
[4]*Key Laboratory for Quantum Materials of Zhejiang Province,*
School of Science, Westlake University, Hangzhou 310024, Zhejiang, China
[5]*Institute of Natural Sciences, Westlake Institute for Advanced Study, Hangzhou 310024, Zhejiang, China*
[6]*Center for Neutron Science and Technology, Guangdong Provincial Key Laboratory of Magnetoelectric Physics and Devices,*
State Key Laboratory of Optoelectronic Materials and Technologies,
School of Physics, Sun Yat-Sen University, Guangzhou, 510275, China

The discovery of high-temperature superconductivity (HTSC) in pressurized La$_3$Ni$_2$O$_7$ has aroused a surge in the exploration of HTSC in the multilayer nickelates. Presently, while HTSC is only found in pressurized circumstance, most of the experimental detections are performed at ambient pressure (AP) due to technical problems. Here we focus on the single-bilayer film of La$_3$Ni$_2$O$_7$ at AP, and propose that an imposed strong perpendicular electric field can strongly enhance its superconducting T_c. The reasons lies as follow. Under strong electric field, the layer with lower potential energy will accept electrons flowing from the other layer to fill in the Ni-$3d_{x^2-y^2}$ orbitals in this layer, as the nearly half-filled Ni-$3d_{z^2}$ orbital in this layer cannot accommodate more electrons. With the enhancement of the filling fraction in the $3d_{x^2-y^2}$ orbitals in this layer, the interlayer s-wave pairing will be subjected to the pair-breaking effect and be suppressed, but the intralayer d-wave pairing in this layer is promptly and strongly enhanced, which mimics the cuprates. Our combined simplified one-orbital study and comprehensive two-orbital one under mean-field treatment consistently verify this idea and yield that an imposed voltage of about $0.1 \sim 0.2$ volt between the two layers is enough to get the HTSC at AP. Our results appeal for experimental verification.

Introduction: The discovery of superconductivity (SC) with critical temperature $T_c \approx 80$ K in the pressurized La$_3$Ni$_2$O$_7$ [1–9] has attracted great interests [10–24]. This discovery has aroused exploration of high-T_c SC (HTSC) in multilayer nickelates, resulting in the discovery of SC in the pressurized La$_4$Ni$_3$O$_{10}$ [25–31], which in together with the previously synthesized infinite-layer nickelates Nd$_{1-x}$Sr$_x$NiO$_2$ [32–35] have established a new superconductors family other than the cuprates and the iron-based superconductors, arousing lots of studies [36–118]. Presently, although various groups have conducted experiments to investigate the properties of La$_3$Ni$_2$O$_7$ [10–24], most of these experiments were conducted at ambient pressure (AP). The circumstance of high pressure not only strongly hinders the experimental detection of the samples, but also brings difficulties in the application of the SC in industry. Therefore, it is eagerly expected that HTSC can be realized in the multilayer nickelates at AP. Here we propose a viable approach to realize HTSC in La$_3$Ni$_2$O$_7$ at AP.

Presently, the pairing mechanism in the pressurized La$_3$Ni$_2$O$_7$ is still under debate [71–97, 101–105]. Density-functional-theory (DFT) based first-principle calculations have suggested that the low-energy orbitals are mainly Ni-$3d_{z^2}$ and $3d_{x^2-y^2}$, which are nearly half- and quarter- filled [1, 40, 41]. Due to the various experiments which have revealed the strongly-correlated characteristic of the material [24, 36], we can take a strong-coupling viewpoint of the system. In this viewpoint, the strong Hubbard repulsion suppresses the coherent motion of the nearly half-filled $3d_{z^2}$ electrons, which can almost be viewed as localized spins. Therefore, the main carrier of SC in the material should be the $3d_{x^2-y^2}$ electrons, which subject to the in-plane superexchange interaction just mimics the 50% hole-doped cuprates. However, the $3d_{z^2}$ orbitals also play an important role through interplaying with the $3d_{x^2-y^2}$ orbitals. The strong interlayer superexchange of the $3d_{z^2}$ electrons [62] provides the pairing potential, which can be transmitted to the $3d_{x^2-y^2}$ electrons through the Hund's rule [76, 77, 79, 89] or the nearest-neighbor (NN) hybridization [62, 80] or both. In such viewpoint, the role of pressure in enhancing the T_c may lie in the enhancement of the interlayer superexchange, the inter-orbital hybridization, or their combination. At AP, the enhancement of these parameters might be realized through chemical element substitution or chemical doping, which is still on the way.

In this work, we propose an alternative approach to realize HTSC in La$_3$Ni$_2$O$_7$ at AP. We focus on the thin film of this material. The La$_3$Ni$_2$O$_7$ film has been synthesized, in which the resonant soft x-ray experiment has revealed spin density wave (SDW) [18]. Here we consider the thinnest limit, i.e. a single bilayer film of La$_3$Ni$_2$O$_7$. The single bilayer film can be grown by using such approaches as the molecular beam epitaxy, the chemical vapor deposition or the pulsed laser deposition. We can
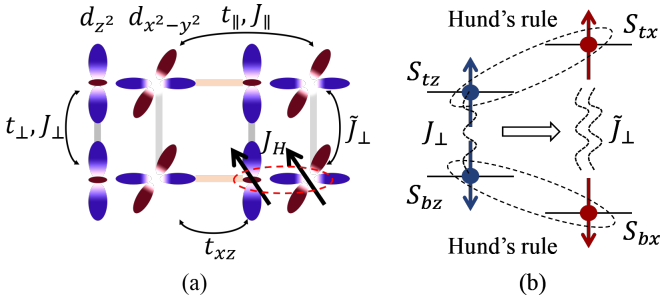
FIG. 1. (a) Schematic diagram for the dominant hopping integrals and superexchange interactions between the E_g orbitals in $La_3Ni_2O_7$. (b) Schematic diagram illustrating that the Hund's rule coupling transmits the interlayer superexchange interaction $J_\perp$ between the $3d_{z^2}$ orbitals to the effective one $\tilde{J}_\perp$ between the $3d_{x^2-y^2}$ orbitals.
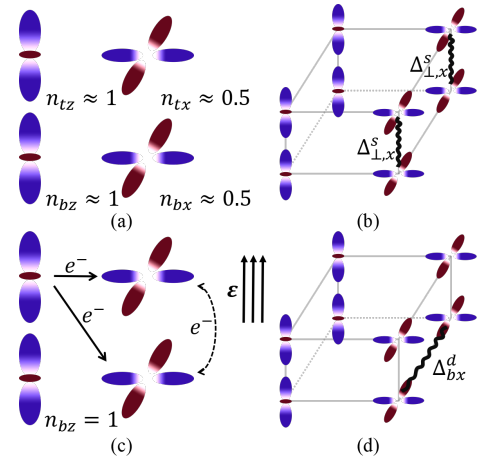

FIG. 2. (a) Filling fractions of the four E_g orbitals within an unit cell without electric field. (b) The dominant pairing configuration for (a). (c) Schematic diagram showing how the electrons flow under the perpendicular electric field ε pointing upward. (d) The dominant pairing configuration for (c).

impose a perpendicular electric field, say pointing upward, in this single bilayer, so that electrons from the top layer will flow to the bottom layer. As the $3d_{z^2}$ orbitals in the bottom layer is already half-filled and thus cannot accommodate more electrons due to the strong Hubbard repulsion, the electrons which flow to the bottom layer have to fill the $3d_{x^2-y^2}$ orbitals. Such enhancement of the filling fraction of the bottom-layer $3d_{x^2-y^2}$ orbitals will first suppress the interlayer s-wave SC due to mismatch of the electron numbers between the two layers, and then promptly lead to the intralayer d-wave HTSC in the bottom layer. To test this idea, we have performed combined simplified single-orbital study and comprehensive two-orbital one, with both studies consistently verify that an voltage of around $0.1 \sim 0.2$ volt between the two layers is enough to induce d-wave HTSC in the bottom layer. Interestingly, the d-wave SC carried by the $3d_{x^2-y^2}$ electrons in the bottom layer coexists with the interlayer s-wave pseudo-gap carried by the $3d_{z^2}$ electrons. Our proposal potentially provides a viable approach to realize HTSC in the single bilayer film of $La_3Ni_2O_7$.

General Consideration and a Simplified Study: Due to the quasi-2D structure of the material, the lattice and electronic structures of the single-bilayer $La_3Ni_2O_7$ film should be near those of the bulk material. The Ni atoms in the AP phase crystal approximately form a bilayer square lattice. As illustrated in Fig. 1 (a), the leading hopping integrals are the interlayer hopping of the d_{z^2} electrons $t_\perp$ and the intralayer nearest-neighbor (NN) hopping of the $d_{x^2-y^2}$ electrons $t_\parallel$. Under strong Hubbard U, these hopping terms can induce the effective superexchange interaction $J_\perp$ and $J_\parallel$ through the relation $J \approx \frac{4t^2}{U}$. Under the Hund's rule coupling J_H, the spins of the two orbitals are inclined to be parallel aligned, as illustrated in Fig. 1 (b), which partly transmits the interlayer superexchange $J_\perp$ between the d_{z^2} orbitals to the $d_{x^2-y^2}$ orbitals as $\tilde{J}_\perp = \alpha J_\perp$ with $\alpha \in (0,1)$. In addition, there exists intralayer NN-bond hybridization

t_{xz} between the two orbitals. As shown in Fig. 2 (a), the quarter-filled $3d_{x^2-y^2}$ electrons subject to the $J_\parallel$ and the $\tilde{J}_\perp$ terms can pair in principle. However, due to the reduced $\tilde{J}_\perp$ and filling fraction at AP, only a weak interlayer pairing of $3d_{x^2-y^2}$ electrons can be obtained [119], as illustrated in Fig. 2 (b).

Now let us turn on the perpendicular electric field ε pointing upward, as shown in Fig. 2 (c) and (d). Under this field, the electrons flow from the top layer to the bottom one. As the $3d_{z^2}$ orbitals in the bottom layer is already nearly half-filled which cannot accommodate more electrons, the majority of the electrons flowing to this layer will fill in the $3d_{x^2-y^2}$ orbitals. In the top layer, since the $3d_{z^2}$ orbitals host larger density of state (DOS) than the $3d_{x^2-y^2}$ orbitals, they will donate most electrons. These donated electrons can flow to the $3d_{x^2-y^2}$ orbitals in the two layers, with more of them to the $3d_{x^2-y^2}$ orbitals in the bottom layer.

Even with doped holes under the electric field, the top-layer $3d_{z^2}$ electrons still cannot carry SC: Firstly, lacking pairing interaction, they cannot form intralayer pairing. Secondly, although they can pair with the localized bottom-layer $3d_{z^2}$ electrons, such pair cannot coherently move, only resulting in pseudo-gap. Therefore, the SC in the presence of ε can only be carried by the $3d_{x^2-y^2}$ orbitals. As the filling fractions of the $3d_{x^2-y^2}$ orbitals in the two layers are different, their Fermi levels are relatively shift, which will suppress their interlayer pairing. The $3d_{x^2-y^2}$ orbitals in the bottom layer will form intralayer d-wave SC, mimicsing the cuprates, as shown in Fig. 2 (d). When the field ε is strong enough so that the filling fraction of the bottom $3d_{x^2-y^2}$ orbitals is near that of the optimal doped cuprates, d-wave HTSC will be achieved in the material.

Based on the above general consideration, we first conduct the following simplified model study including only the $3d_{x^2-y^2}$-orbital, with the $3d_{z^2}$ orbital only viewed as a source which tunes the total electron number. The widely adopted single $3d_{x^2-y^2}$-orbital bilayer $t-J-J_\perp$ model [76, 77, 79, 89] is adopted, which reads,

$$H = - t_\parallel \sum_{\langle i,j\rangle,\mu,\sigma} \left(c_{i\mu\sigma}^\dagger c_{j\mu\sigma} + \text{h.c.} \right) + \sum_{i,\mu} \epsilon_\mu n_{i\mu}$$
$$+ J_\parallel \sum_{\langle i,j\rangle,\mu} \boldsymbol{S}_{i\mu} \cdot \boldsymbol{S}_{j\mu} + \tilde{J}_\perp \sum_i \boldsymbol{S}_{it} \cdot \boldsymbol{S}_{ib}. \quad (1)$$

Here $c_{i\mu\sigma}^\dagger$ creates an electron at site i in the layer μ (=top (t)/bottom (b)) with spin σ, and $n_{i\mu}$ or $\boldsymbol{S}_{i\mu}$ denote the corresponding electron number or spin operator. Only NN- bond $\langle i,j\rangle$ is considered in the summation. The layer-dependent chemical potential ϵ_μ is introduced to control the filling fractions of the two layers under the imposed ε. We assume that the ratio between the electron number flowing from the $3d_{z^2}$ orbitals and that flowing from $3d_{x^2-y^2}$ orbitals in the top layer is 2 : 1 due to reason of DOS. Fixing the filling fractions under this assumption, we solve the model with standard SBMF theory [120]. See more details in the SM.
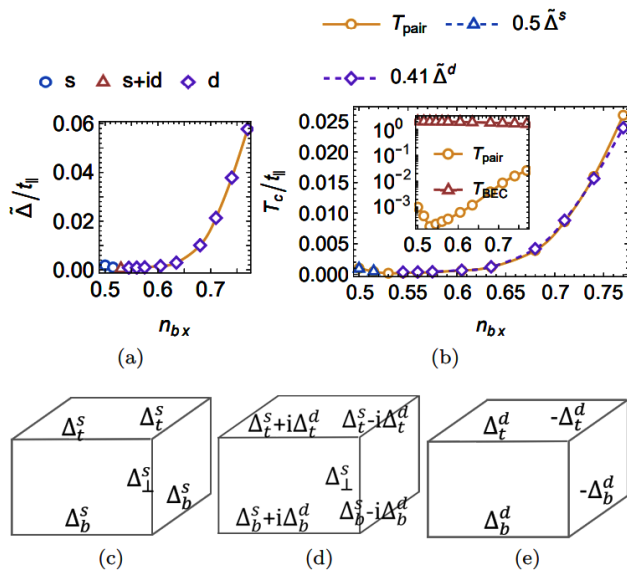

FIG. 3. (a) The pairing amplitude $\tilde{\Delta}$ (in unit of $t_\parallel$) as function of the bottom-layer filling fraction n_{bx}. Different pairing symmetries are marked by different colors. (b) The T_c as function of n_{bx}, in comparison with $0.41\tilde{\Delta}$ for the d-wave and $0.5\tilde{\Delta}$ for the s-wave regime. Inset: the spinon pairing temperature T_{pair} and the holon condensation temperature T_{BEC} as function of n_{bx}. In (a,b), we set $J_\parallel = 0.4t_\parallel$ and $\tilde{J}_\perp = (1-\delta_{tz}) \times 1.8J_\parallel$. (c)-(e) The pairing configurations of the s-wave, (s+id)-wave, and d-wave, respectively.

The main results of our SBMF theory are shown in Fig. 3. Fig. 3(a) shows the amplitude and symmetry of the ground-state pairing gap as function of the bottom-layer $3d_{x^2-y^2}$ electron number n_{bx}, whose value enhances with ε. It is shown that when n_{bx} enhances, the pairing gap amplitude $\tilde{\Delta}$ decays first and then increases. When $n_{bx} \in (0.5, 0.515)$, the ground state is interlayer s-wave pairing. The $\tilde{\Delta}$ decreases with the enhancement of ε or n_{bx} in this regime because the mismatch of the Fermi surfaces (FSs) of the two layers caused by ε suppresses the interlayer pairing, similar to the case of a singlet pairing state placed within a pair-breaking Zeeman field. When $n_{bx} \geq 0.545$, the ground state is an intralayer d-wave SC, similar to the case of the cuprates. It is inspiring that with the enhancement of n_{bx} in this regime, the $\tilde{\Delta}$ enhances promptly, similar to the case in the overdoped cuprates, wherein the enhancement of the filling fraction promptly enhances the pairing strength. When n_{bx} is near 0.53, the ground state is an s+id-wave SC. The real-space pairing configurations of the three different pairing symmetries are illustrated in Fig. 3(c-e).

The T_c as a function of n_{bx} is shown in Fig. 3(b). In the SBMF theory, the T_c is given as the lower one between the spinon-pairing temperature T_{pair} and the holon-BEC temperature T_{BEC}, see the SM. The inset of Fig. 3(b) displays $T_{\text{BEC}} \gg T_{\text{pair}}$, rendering $T_c = T_{\text{pair}}$ in the considered n_{bx} regime. A comparison between Fig. 3(b) and (a) suggests that T_c scales with $\tilde{\Delta}$, which is more clear when the $T_c \sim n_{bx}$ is well fitted by $0.41\tilde{\Delta} \sim n_{bx}$ for the d-wave and $0.5\tilde{\Delta} \sim n_{bx}$ for the s-wave in Fig. 3(b), consistent with the BCS theory. It is inspiring that in the regime $n_{bx} \geq 0.75$, the $T_c \approx 0.02t_\parallel \approx 0.01$ eV≈ 100 K, suggesting that HTSC can be achieved by tuning ε.

On the above, we have adopted $\tilde{J}_\perp = \alpha J_\perp (1-\delta_{tz})$ with $\alpha = 1$, where δ_{tz} denotes the hole density of the top-$3d_{z^2}$ orbital. When α is reduced by quantum fluctuation, only the low-n_{bx} regime accommodating the interlayer s-wave or $s+id$-wave pairing in Fig. 3(a, b) shrinks but the high-n_{bx} regime accommodating the intralayer d-wave HTSC is not affected because the intralayer pairing is blind to $\tilde{J}_\perp$. Furthermore, assuming different ratios between the changes of the filling fractions of the three E_g orbitals turns out to yield similar results, as the dominant pairing in this system is the intra-bottom-layer pairing under strong ε, which is blind to the filling fraction of the top layer. See the SM for details.

The comprehensive two-orbital study: The above simplified single-orbital study has obvious drawbacks: We do not know the concrete relation between the strength ε of the exerted electric field and the changes of the filling fractions of the three E_g orbitals in the La$_3$Ni$_2$O$_7$ bilayer. Nor do we know how the neglected $3d_{z^2}$ orbital degree of freedom affects the pairing nature of the system. To settle these puzzles, we conduct a comprehensive two-orbital study for the problem. The Hamiltonian reads,

$$H = - t_{\parallel} \sum_{\langle i,j \rangle, \mu} \left(c^{\dagger}_{i\mu x\sigma} c_{j\mu x\sigma} + \text{h.c.} \right) - t_{\perp} \sum_{i} \left(c^{\dagger}_{itz\sigma} c_{ibz\sigma} + \text{h.c.} \right) - t_{xz} \sum_{\langle i,j \rangle \mu} \left(c^{\dagger}_{i\mu x\sigma} c_{j\mu z\sigma} + (z \leftrightarrow x) + \text{h.c.} \right)$$

$$+ J_{\parallel} \sum_{\langle i,j \rangle \mu} \boldsymbol{S}_{i\mu x} \cdot \boldsymbol{S}_{j\mu x} + J_{\perp} \sum_{i} \boldsymbol{S}_{itz} \cdot \boldsymbol{S}_{ibz} + \tilde{J}_{\perp} \sum_{i} \boldsymbol{S}_{itx} \cdot \boldsymbol{S}_{ibx} + \epsilon_z \sum_{i\mu\sigma} n_{i\mu z\sigma} + \epsilon_x \sum_{i\mu\sigma} n_{i\mu x\sigma}$$

$$+ \frac{\varepsilon}{2} \sum_{i\alpha\sigma} n_{it\alpha\sigma} - \frac{\varepsilon}{2} \sum_{i\alpha\sigma} n_{ib\alpha\sigma} \tag{2}$$

The operators $c_{i\mu\alpha\sigma}$, $n_{i\mu\alpha}$, $\boldsymbol{S}_{i\mu\alpha}$ take the same meanings as those in model (1) except that one more index $\alpha = x/z$ appears which labels the orbital. Note that $\boldsymbol{S}_{i\mu\alpha}$ for each orbital α is spin-$\frac{1}{2}$ operator. ϵ_x and ϵ_z denote the on-site energy of the two orbitals. While the TB parameters are obtained from the DFT calculations for bulk $La_3Ni_2O_7$ at AP [119], the superexchange interactions are obtained through the relation $J \approx 4t^2/U$, with $U = 5$ eV. Finally ε denotes the voltage between the two layers caused by the imposed electric field.

The main results of the SBMF treatment of (2) (see the SM) is shown in Fig. 4. Fig. 4(a) shows the ε-dependence of the hole densities $\delta_{\mu\alpha}$. Obviously, the δ_{tz} enhances obviously with ε, suggesting that the top-$3d_{z^2}$ orbital is donating electrons. These donated electrons flow to the $3d_{x^2-y^2}$ orbitals in the two layers, with more of them flowing to the bottom layer. Fig. 4(b) shows the ε-dependence of the pairing symmetry and the pairing gap amplitude of the bottom-layer $3d_{x^2-y^2}$ orbital. At low $\varepsilon \leq 0.02$ eV, the pairing symmetry is s-wave, whose pairing configuration is shown in Fig. 4(c), wherein the d_{z^2}-orbital form interlayer s-wave pseudo-gap, while the $d_{x^2-y^2}$ orbital form s-wave SC with coexisting intralayer and interlayer pairing. In this regime the SC is suppressed by the enhancement of ε. When $\varepsilon > 0.02$ eV, the pairing symmetry is $d(d_{x^2-y^2}) + is(d_{z^2})$, whose pairing configuration is shown in Fig. 4(d). In this state, the $3d_{z^2}$ orbital form interlay s-wave pseudo-gap, while the bottom-layer $3d_{x^2-y^2}$ orbital form intralayer d-wave SC. When ε enhances in this regime, the pairing amplitude for the bottom-layer $3d_{x^2-y^2}$ orbitals enhances promptly. For $\varepsilon > 0.13$ eV, the pairing amplitude can arrive at 0.02 eV. Then from the relation $T_c \approx 0.41\Delta$ for the d-wave SC illustrated in Fig. 3(b), we have $T_c \approx 80$ K!

The main result shown in Fig. 4(b) for the comprehensive two-orbital study and that shown in Fig. 3(b) for the simplified one-orbital study look similar, except that in Fig. 4(b) the result is expressed as function of the imposed electric field ε which is directly controllable. Actually, if we replace the x-axis of Fig. 4(b) by the calculated $n_{bx} = 1 - \delta_{bx}$, the resulting curve nearly coincides with Fig. 3(b), particularly in the large-n_{bx} regime, see the SM. The main reason for such similarity lies in that under strong electric field, the dominant superconducting pairing is the intra-bottom-layer $3d_{x^2-y^2}$-orbital pairing, which is not seriously affected by the $3d_{z^2}$ orbital degree

of freedom. The main new information obtained in the two-orbital study lies in that the $3d_{z^2}$ orbital form interlayer s-wave pseudo-gap which coexists with the intra-bottom-layer d-wave HTSC of the $3d_{x^2-y^2}$ orbital, as shown in Fig. 4(d). The $1 : i$ mixing of the two pairing gap leads to time-reversal-symmetry-breaking, although the experimentally detected superconducting gap is the standard d-wave gap of the $3d_{x^2-y^2}$ orbital. This intriguing result is left for experimental verification.
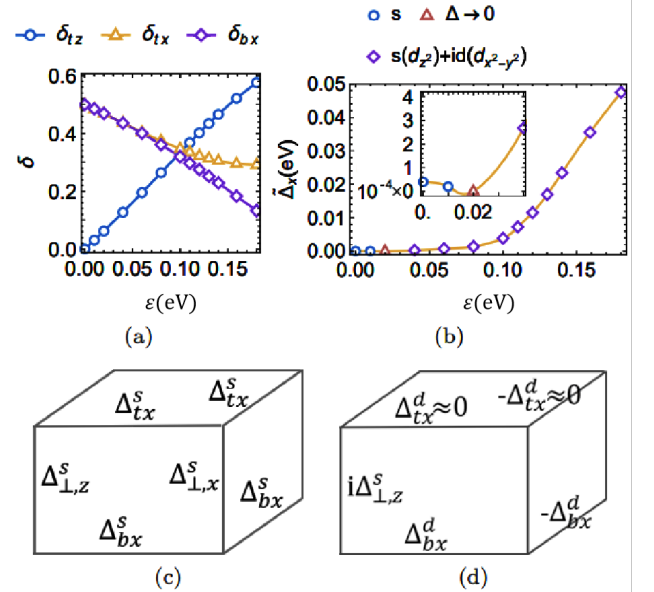

FIG. 4. (a) The hole densities $\delta_{\mu\alpha}$ for the three orbitals as functions of the strength of the electric field ε. (b) The pairing gap amplitude of the bottom-layer $3d_{x^2-y^2}$-orbital as function of ε. Inset: zooming in of the low-ε regime. (c)-(d) The pairing configurations of the s-wave and the $s(d_{z^2})+id(d_{x^2-y^2})$-wave, respectively.

Conclusion and Discussion: In conclusion, we propose that an imposed strong perpendicular electric field can enhance the superconducting T_c of the single-bilayer film of $La_3Ni_2O_7$ at AP. The reason lies in that under the strong electric field, the electrons in the layer with higher potential energy will flow to the layer with lower potential energy, to fill the $3d_{x^2-y^2}$ orbitals in the latter layer. With considerably enhanced filling fraction, the $3d_{x^2-y^2}$ electrons in that layer just mimics the cuprates, which form intralayer d-wave HTSC. Our combined one-orbital

and two-orbital studies consistently verify this idea. Our results predict that when the imposed voltage between the two layers is stronger than $0.1 \sim 0.2$ eV, the resulted T_c can go beyond the boiling point of liquid nitrogen.

In our calculations, we have adopted the TB parameters from the DFT calculations for bulk $La_3Ni_2O_7$ at AP, which might be slightly different from those for the single-bilayer film. However, the strong-coupling calculations performed here do not seriously rely on the accurate values of these parameters, because the main physics here is very simple. Actually, the well consistency between the result of the comprehensive two-orbital study and those of the simplified one-orbital studies with assuming different input conditions just verifies the robustness of our conclusion.

Appendix A: Slave-boson mean-field treatment of the one-orbital model

In the one-orbital model, we begin with the Hamiltonian

$$H = -t_{\parallel} \sum_{\langle i,j \rangle, \mu, \sigma} \left(c^{\dagger}_{i\mu\sigma} c_{j\mu\sigma} + \text{h.c.} \right) + \sum_{i,\mu} \epsilon_{\mu} n_{i\mu} + J_{\parallel} \sum_{\langle i,j \rangle, \mu} \boldsymbol{S}_{i\mu} \cdot \boldsymbol{S}_{j\mu} + \tilde{J}_{\perp} \sum_{i} \boldsymbol{S}_{it} \cdot \boldsymbol{S}_{ib}, \tag{S1}$$

where $c^{\dagger}_{i\mu\sigma}$ creates a electron in the $d_{x^2-y^2}$ orbital with the spin $\sigma = \{\uparrow, \downarrow\}$ at the lattice site i in the layer $\mu = \{t, b\}$. $n_{i\mu} = \sum_{\sigma} c^{\dagger}_{i\mu\sigma} c_{i\mu\sigma}$ is the particle number operator. $\boldsymbol{S}_{i\mu} = \frac{1}{2} c_{i\mu\sigma} [\boldsymbol{\sigma}]_{\sigma\sigma'} c_{i\mu\sigma'}$ is the spin operator with Pauli matrix $\boldsymbol{\sigma} = (\sigma_x, \sigma_y, \sigma_z)$. Here we set $t_{\parallel} = 1$ as the unit, and the intra-layer and interlayer spin exchage are given by $J_{\parallel} = 0.4 t_{\parallel}$ and $\tilde{J}_{\perp} \approx \alpha J_{\perp} (1 - \delta_{tz})$ with $\alpha = 1$, where δ_{tz} denotes the hole density of the top-$3d_{z^2}$ orbital. Suppose each top-layer $3d_{z^2}$ or $3d_{x^2-y^2}$ orbital denotes electrons with number δ or η_1 in average, then each bottom-layer $3d_{x^2-y^2}$ orbital will accept electrons with number $\eta_2 = \delta + \eta_1$. Therefore, the filling fraction of the top or bottom layer in model (S1) should be $\frac{1}{2} - \eta_1$ or $\frac{1}{2} + \eta_2$. ϵ_{μ} corresponding to chemical potential is consistently derived from δ.

In this simplified single-orbital study, we cannot determine the concrete relation between ε and δ or $\eta_{1,2}$. But clearly, δ and η_1 enhance with the enhancement of ε. The particle number of the bottom-layer d_{z^2} orbital is near half-filling without external electric field, thus in the strong-coupling limit, the bottom-layer d_{z^2} orbital approaches half-filling and becomes incapable of accommodating additional electrons, even under a small perpendicular electric field. Therefore we fix the particle number of the bottom-layer d_{z^2} orbital $n_{bz} = 1$. Considering that the electrons flow from the top layer only to the bottom layer $d_{x^2-y^2}$ orbital, we express the particle number of the top-layer d_{z^2} orbital, the top-layer $d_{x^2-y^2}$ orbital and the bottom layer $d_{x^2-y^2}$ orbital as $n_{tz} = 1 - \delta$, $n_{tx} = 0.5 - \eta_1$ and $n_{bx} = 0.5 + \delta + \eta_1$ respectively.

To get the knowledge of η_1/δ in different perpendicular electric field, we solve the tight-binding (TB) Hamiltonian with the parameters from Liu et al's work and an additional external electric field term $(\varepsilon/2) \sum_{i,\alpha,\sigma} (n_{it\alpha\sigma} - n_{ib\alpha\sigma})$. We plot the (δ, η_1) points (Fig. A1), finding that $\eta_1/\delta \approx 1/2$. Thus we assume $\eta_1/\delta = 1/2$ (i.e. $(n_{tx} - 0.5)/(n_{bx} - 0.5) = -\eta_1/\eta_2 = -1/3$) in the one-orbital model study.
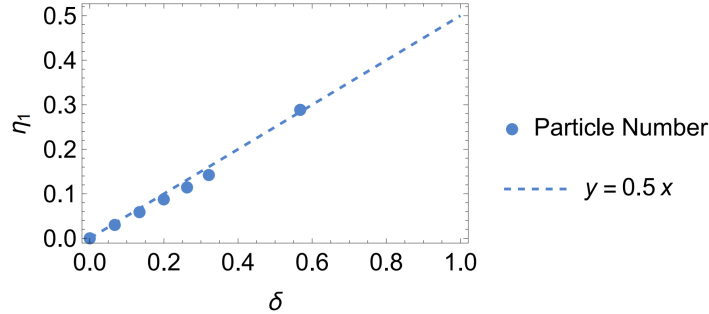

FIG. A1. The change of electron number δ and η_1 under different electric field. The results are represented by the dots (δ, η_1). All of the dots are near the $y = 0.5x$ line (dashed line), indicating that $\eta_1 \approx 0.5\delta$.

We solve the Hamiltonian in Eq. (S1) by slave-boson mean-field (SBMF) theory. The electron operator (c) is decomposed into the product of a fermionic spinon operator (f) and a bosonic holon operator (b), i.e. $c^{\dagger}_{i\mu\sigma} = f^{\dagger}_{i\mu\sigma} b_{i\mu}$. The mean-field Hamiltonian of spinon and holon can be expressed as

$$\begin{aligned}
H_{\text{spinon}} = &- t_{\parallel} \sum_{\langle i,j \rangle, \mu, \sigma} \left(\left\langle b_{i\mu} b^{\dagger}_{j\mu} \right\rangle f^{\dagger}_{i\mu\sigma} f_{j\mu\sigma} + \text{h.c.} \right) + \sum_{i,\mu,\sigma} \epsilon_{\mu} f^{\dagger}_{i\mu\sigma} f_{i\mu\sigma} \\
&- \frac{3}{8} J_{\parallel} \sum_{\langle i,j \rangle, \mu} \left(\langle \chi^{\dagger}_{\mu} \rangle \chi_{ij,\mu} + \text{h.c.} + \langle \Delta^{\dagger}_{\mu} \rangle \Delta_{ij,\mu} + \text{h.c.} - \langle \chi^{\dagger}_{\mu} \rangle \langle \chi_{\mu} \rangle - \langle \Delta^{\dagger}_{\mu} \rangle \langle \Delta_{\mu} \rangle \right) \\
&- \frac{3}{8} (1 - \delta) J_{\perp} \sum_{i} \left(\langle \chi^{\perp\dagger} \rangle \chi^{\perp}_{i} + \text{h.c.} + \langle \Delta^{\perp\dagger} \rangle \Delta^{\perp}_{i} + \text{h.c.} - \langle \chi^{\perp\dagger} \rangle \langle \chi^{\perp} \rangle - \langle \Delta^{\perp\dagger} \rangle \langle \Delta^{\perp} \rangle \right)
\end{aligned} \tag{S2}$$

and

$$H_{\text{holon}} = -t_{\parallel} \sum_{\langle i,j \rangle, \mu} \left(\langle \chi_{ij,\mu} \rangle b^{\dagger}_{i\mu} b_{j\mu} + \text{h.c.} \right) \tag{S3}$$

where $\langle b_{i\mu} \rangle = \left\langle b_{i\mu}^\dagger \right\rangle = \sqrt{\delta_\mu}$ is sustained below the holon condensation temperature, and the bonding and pairing order parameters are defined as

$$
\begin{aligned}
&\chi_{ij,\mu}^\dagger = \sum_\sigma f_{i\mu\sigma}^\dagger f_{j\mu\sigma}, \chi_\mu^\dagger = \frac{1}{2N} \sum_{\langle i,j \rangle} \chi_{ij,\mu}^\dagger, \\
&\chi_i^{\perp\dagger} = \sum_\sigma f_{it\sigma}^\dagger f_{ib\sigma}, \chi^{\perp\dagger} = \frac{1}{N} \sum_i \chi_i^{\perp\dagger}, \\
&\Delta_{ij,\mu}^\dagger = f_{i\mu\uparrow}^\dagger f_{j\mu\downarrow}^\dagger - f_{i\mu\downarrow}^\dagger f_{j\mu\uparrow}^\dagger, \Delta_\mu^{\boldsymbol{x}} = \frac{1}{2N} \sum_{\langle i,j \rangle} \Delta_{ij,\mu}, \\
&\Delta_i^{\perp\dagger} = f_{it\uparrow}^\dagger f_{ib\downarrow}^\dagger - f_{it\downarrow}^\dagger f_{ib\uparrow}^\dagger, \Delta^\perp = \frac{1}{N} \sum_i \Delta_i^\perp
\end{aligned}
\tag{S4}
$$

In the mean-field approach, we constrain the particle number and obtain the expectation value of the mean-field order parameters at zero temperature by solving the self-consistent equations derived from Eq. (S2).

$$
\begin{aligned}
&\delta_\mu = 1 - \frac{1}{N} \sum_k \left(\langle c_{k\mu\uparrow}^\dagger c_{k\mu\uparrow} \rangle + \langle c_{-k\mu\downarrow}^\dagger c_{-k\mu\downarrow} \rangle \right), \ \delta_t = 0.5 + \eta_1, \ \delta_b = 0.5 - \eta_2 \\
&\langle \chi_\mu \rangle = \frac{1}{2N} \sum_{\langle i,j \rangle} \langle \chi_{ij,\mu} \rangle = \frac{1}{N} \sum_k \frac{\cos(k_x) + \cos(k_y)}{2} \left(\langle c_{k\mu\uparrow}^\dagger c_{k\mu\uparrow} \rangle + \langle c_{-k\mu\downarrow}^\dagger c_{-k\mu\downarrow} \rangle \right), \\
&\langle \chi^\perp \rangle = \frac{1}{N} \sum_i \langle \chi_i^\perp \rangle = \frac{1}{N} \sum_k \left(\langle c_{kt\uparrow}^\dagger c_{kb\uparrow} \rangle + \langle c_{-kt\downarrow}^\dagger c_{-kb\downarrow} \rangle \right), \\
&\langle \Delta_\mu^{\boldsymbol{x}} \rangle^* = \frac{1}{2N} \sum_{\langle i,j \rangle} \langle \Delta_{ij,\mu} \rangle^* = \frac{1}{N} \sum_k 2\cos(k_x) \langle c_{k\mu\uparrow}^\dagger c_{-k\mu\downarrow}^\dagger \rangle, \\
&\langle \Delta^\perp \rangle^* = \frac{1}{N} \sum_i \langle \Delta_i^\perp \rangle^* = \frac{2}{N} \sum_k \langle c_{kt\uparrow}^\dagger c_{-kb\downarrow}^\dagger \rangle
\end{aligned}
\tag{S5}
$$

From Eq. (S5), we can also determine the spinon-pairing temperature T_{pair} by solving for the critical condition $\Delta = 0$ at finite temperature.

To characterize the pairing type of the system, the pairing gap amplitude $\tilde{\Delta}$ is defined as the maximal value of the pairing gaps. For the interlayer s-wave pairing, $\tilde{\Delta} = -\frac{3}{8} \tilde{J}_\perp \left\langle \Delta^\perp \right\rangle$. For the d-wave pairing, $\tilde{\Delta}_x = -\frac{3}{2} J_\parallel \left\langle \Delta_b^{\boldsymbol{x}} \right\rangle$.

The holon condensation temperature can be calculated according to the Berezinskii-Kosterlitz-Thouless (BKT) transition theory. The holon operator can be written as $b_{i\mu}^\dagger = \sqrt{\delta_\mu} e^{i\theta_\mu(i)}$, whose phase fluctuations lead to the BKT transition. Then the holon Hamiltonian can be written as a XY-model-like form

$$
H_{\text{holon}} = -2t_\parallel \sum_{\langle i,j \rangle, \mu} \langle \chi_\mu \rangle \delta_\mu \cos(\theta_\mu(i) - \theta_\mu(j))
\tag{S6}
$$

We transform the model to a continuous model

$$
H_{\text{holon}} \sim \frac{1}{2} \rho \int \mathrm{d}^2 \boldsymbol{r} \left| \nabla \theta \right|^2
\tag{S7}
$$

where

$$
\rho = \sum_{|\boldsymbol{l}|=1} \sum_\mu t_\parallel \langle \chi_\mu \rangle \delta_\mu l^2
\tag{S8}
$$

is the superfluid stiffness. Then we can get T_{BEC} from the relationship $T_{\text{BEC}} = (\pi/2)\rho$.

Considering that the real η_1/δ may be different from the TB results, we also study the $\eta_1/\delta = 0/1$ and $\eta_1/\delta = -1/2$ situations (i.e. $(n_{tx} - 0.5)/(n_{bx} - 0.5) = 0/1$ and $(n_{tx} - 0.5)/(n_{bx} - 0.5) = 1/2$). We find that the phase diagrams of different $(n_{tx} - 0.5)/(n_{bx} - 0.5)$ are similar to each other (shown in Fig. A2 (a)-(c)). Additionally, the dimensionless d-wave pairing gap $\Delta^d (= \Delta_b^{\boldsymbol{x}})$ is only determined by the particle number n_{bx} but is not related to the particle number ratio $(n_{tx} - 0.5)/(n_{bx} - 0.5)$ (shown in Fig. A2 (d)).
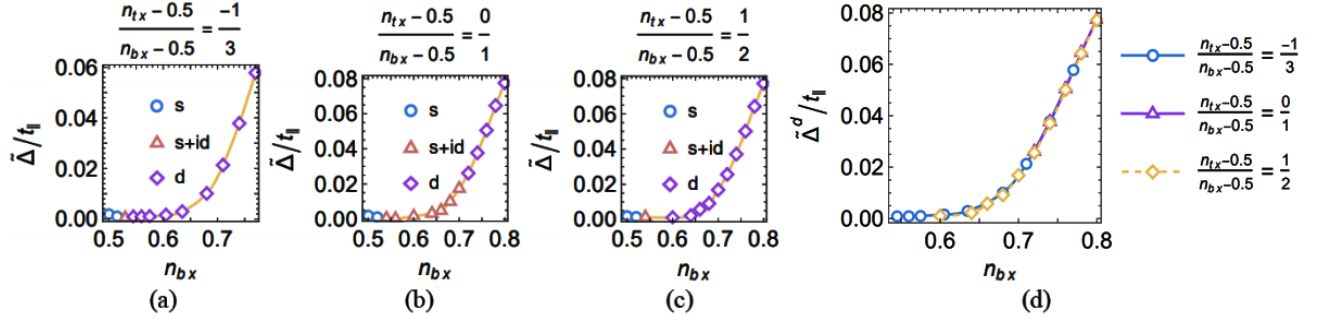
FIG. A2. (a)-(c) The pairing amplitude $\tilde{\Delta}$ (in unit of $t_\parallel$) as function of the bottom-layer particle number n_{bx} controlled by the imposed electric field. Different pairing symmetry is marked by different colors. (d) The d-wave pairing gap $\tilde{\Delta}^d$ of different particle number ratios as function of particle number n_{bx} (represented by different lines). The lines almost coincide with each other, indicating that the dimensionless d-wave pairing gap is only determined by the particle number n_{bx}.

Appendix B: Slave-boson mean-field treatment of the two-orbital model

In the two-orbital model, the Hamiltonian takes the form

$$
\begin{aligned}
H = & -t_\parallel \sum_{\langle i,j \rangle,\mu} \left(c^\dagger_{i\mu x\sigma} c_{j\mu x\sigma} + \text{h.c.} \right) - t_\perp \sum_i \left(c^\dagger_{itz\sigma} c_{ibz\sigma} + \text{h.c.} \right) - t_{xz} \sum_{\langle i,j \rangle \mu} \left(c^\dagger_{i\mu x\sigma} c_{j\mu z\sigma} + (z \leftrightarrow x) + \text{h.c.} \right) \\
& + J_\parallel \sum_{\langle i,j \rangle \mu} \boldsymbol{S}_{i\mu x} \cdot \boldsymbol{S}_{j\mu x} + J_\perp \sum_i \boldsymbol{S}_{itz} \cdot \boldsymbol{S}_{ibz} + \tilde{J}_\perp \sum_i \boldsymbol{S}_{itx} \cdot \boldsymbol{S}_{ibx} + \epsilon_z \sum_{i\mu\sigma} n_{i\mu z\sigma} + \epsilon_x \sum_{i\mu\sigma} n_{i\mu x\sigma} \\
& + \frac{\varepsilon}{2} \sum_{i\alpha\sigma} n_{it\alpha\sigma} - \frac{\varepsilon}{2} \sum_{i\alpha\sigma} n_{ib\alpha\sigma}
\end{aligned}
\tag{S9}
$$

where $c^\dagger_{i\mu z\sigma}/c^\dagger_{i\mu x\sigma}$ creates a $d_{z^2}/d_{x^2-y^2}$-orbital electron with the spin $\sigma = \{\uparrow, \downarrow\}$ at the lattice site i in the layer $\mu = \{t, b\}$. $n_{i\mu\alpha\sigma} = c^\dagger_{i\mu\alpha\sigma} c_{i\mu\alpha\sigma}$ is the particle number operator for the two E_g orbitals with $\alpha = \{z, x\}$. $\boldsymbol{S}_{i\mu x} = \frac{1}{2} c_{i\mu x\sigma} [\boldsymbol{\sigma}]_{\sigma\sigma'} c_{i\mu x\sigma'}$ is the spin operator with Pauli matrix $\boldsymbol{\sigma} = (\sigma_x, \sigma_y, \sigma_z)$. ϵ_z and ϵ_x represent the equivalent onsite energies of the d_{z^2} and $d_{x^2-y^2}$ orbitals respectively, as determined by the self-consistent equations.

To compare the ground-state energies of different pairing modes, we consider the Hamiltonian with Lagrange multipliers

$$
\tilde{H} = H + (\epsilon_{z0} - \epsilon_z) \sum_{i\mu\sigma} n_{i\mu z\sigma} + (\epsilon_{x0} - \epsilon_x) \sum_{i\mu\sigma} n_{i\mu x\sigma}
\tag{S10}
$$

We adopt the data from the DFT calculations as physical parameters for $\tilde{H}$. The hopping parameters are given by $t_\parallel = 0.400\text{eV}$, $t_{xz} = 0.201\text{eV}$ and $t_\perp = 0.597\text{eV}$. The onsite energies are set to $\epsilon_{z0} = 8.7026\text{eV}$ and $\epsilon_{x0} = 9.2609\text{eV}$. We estimate the spin couplings as $J_\parallel = 0.4t_\parallel$, $J_\perp = 1.8J_\parallel$ and $\tilde{J}_\perp = 0.5J_\perp$.

In the mean-field approximation, each superexchange term in (S9) is also decomposed in $\chi - \Delta$ channel, similar to the single-orbital model. The mean-field Hamiltonian is described as

$$
\begin{aligned}
H_{\text{MF}} = & -t_\parallel \sum_{\langle i,j \rangle,\mu} \delta_{\mu x} \left(c^\dagger_{i\mu x\sigma} c_{j\mu x\sigma} + \text{h.c.} \right) - t_{xz} \sqrt{\delta_{tx} \delta_{tz}} \sum_{\langle i,j \rangle} \left(c^\dagger_{itx\sigma} c_{jtz\sigma} + c^\dagger_{itz\sigma} c_{jtx\sigma} + \text{h.c.} \right) \\
& - \frac{3}{8} J_\parallel \sum_{\langle i,j \rangle \mu} \left(\chi^\dagger_{ij,\mu x} \langle \chi_{\mu x} \rangle + \text{h.c.} + \Delta^\dagger_{ij,\mu x} \langle \Delta_{\mu x} \rangle + \text{h.c.} - \langle \chi^\dagger_{\mu x} \rangle \langle \chi_{\mu x} \rangle - \langle \Delta^\dagger_{\mu x} \rangle \langle \Delta_{\mu x} \rangle \right) \\
& - \frac{3}{8} J_\perp \sum_i \left(\chi^{\perp\dagger}_{iz} \langle \chi^\perp_z \rangle + \text{h.c.} + \Delta^{\perp\dagger}_{iz} \langle \Delta^\perp_z \rangle + \text{h.c.} - \langle \chi^{\perp\dagger}_z \rangle \langle \chi^\perp_z \rangle - \langle \Delta^{\perp\dagger}_z \rangle \langle \Delta^\perp_z \rangle \right) \\
& - \frac{3}{8} \tilde{J}_\perp \sum_i \left(\Delta^{\perp\dagger}_{ix} \langle \Delta^\perp_x \rangle + \text{h.c.} - \langle \Delta^{\perp\dagger}_x \rangle \langle \Delta^\perp_x \rangle \right) \\
& + \epsilon_z \sum_{i\mu\sigma} n_{i\mu z\sigma} + \epsilon_x \sum_{i\mu\sigma} n_{i\mu x\sigma} + \frac{\varepsilon}{2} \sum_{i\alpha\sigma} n_{it\alpha\sigma} - \frac{\varepsilon}{2} \sum_{i\alpha\sigma} n_{ib\alpha\sigma}
\end{aligned}
\tag{S11}
$$

where $\delta_{\mu\alpha} = 1 - \frac{1}{N}\sum_{i\sigma}\langle n_{i\mu\alpha\sigma}\rangle$ is the expected number of holes. Under the electric field, we have $\delta_{bz} = 0$ and δ_{tz}, δ_{tx} and δ_{bx} are solved self-consistently. The mean-field order parameters are represented by

$$
\begin{aligned}
&\chi_{ij,\mu x} = \sum_{\sigma} c^{\dagger}_{i\mu x\sigma}c_{j\mu x\sigma}, \ \ \chi_{\mu x} = \frac{1}{2N}\sum_{\langle i,j\rangle}\chi_{ij,\mu x}, \\
&\chi^{\perp\dagger}_{iz} = \sum_{\sigma} c^{\dagger}_{izt\sigma}c_{izb\sigma}, \ \ \chi^{\perp}_{z} = \frac{1}{N}\sum_{i}\chi^{\perp}_{iz}, \\
&\Delta^{\dagger}_{ij,\mu\alpha} = c^{\dagger}_{i\mu\alpha\uparrow}c^{\dagger}_{j\mu\alpha\downarrow} - c^{\dagger}_{i\mu\alpha\downarrow}c^{\dagger}_{j\mu\alpha\uparrow}, \ \ \Delta^{\boldsymbol{x}}_{\mu x} = \frac{1}{2N}\sum_{\langle i,j\rangle}\Delta_{ij,\mu x}, \\
&\Delta^{\perp\dagger}_{i\alpha} = c^{\dagger}_{it\alpha\uparrow}c^{\dagger}_{ib\alpha\downarrow} - c^{\dagger}_{ib\alpha\downarrow}c^{\dagger}_{it\alpha\uparrow}, \ \ \Delta^{\perp}_{\alpha} = \frac{1}{N}\sum_{i}\Delta^{\perp}_{i\alpha}
\end{aligned} \tag{S12}
$$

Notably, the spin-exchange $\tilde{J}_{\perp}$ of the Hamiltonian in Eq. (S9) doesn't produce a hopping term $\chi^{\perp}_{x}$ in Eq. (S11), which is the feature of such a bilayer system. Without interlayer hopping, a small interlayer spin-exchange $J_{\perp}$ leads to $\langle\chi^{\perp}\rangle \approx 0$.

Consequently, the d_{z^2} orbital only participate in the interlayer pairing. However, this pairing is not SC as the corresponding SC order parameter goes to zero in the SBMF theory due to $\delta_{bz} = 0$. The SC is carried by the $3d_{x^2-y^2}$ orbitals, which can form both intralayer and interlayer pairing. The superconducting T_c scales with the ground state gap amplitude of the $3d_{x^2-y^2}$ orbitals via the BCS relation exhibited in Fig. 3(b) in the main text.

The expectation value of the mean-field order parameters are obtained by numerically solving the following self-consistent equation

$$
\begin{aligned}
&\delta_{\mu\alpha} = 1 - \frac{1}{N}\sum_{k}\left(\langle c^{\dagger}_{k\mu\alpha\uparrow}c_{k\mu\alpha\uparrow}\rangle + \langle c^{\dagger}_{-k\mu\alpha\downarrow}c_{-k\mu\alpha\downarrow}\rangle\right), \ \ \delta_{tz} = 0, \ \ \sum_{\mu\alpha}\delta_{\mu\alpha} = 1, \\
&\langle\chi_{\mu x}\rangle = \frac{1}{N}\sum_{\langle i,j\rangle}\langle\chi_{ij,\mu x}\rangle = \frac{1}{N}\sum_{k}\frac{\cos(k_x) + \cos(k_y)}{2}\left(\langle c^{\dagger}_{k\mu x\uparrow}c_{k\mu x\uparrow}\rangle + \langle c^{\dagger}_{-k\mu x\downarrow}c_{-k\mu x\downarrow}\rangle\right), \\
&\langle\chi^{\perp}_{z}\rangle = \frac{1}{2N}\sum_{i}\langle\chi^{\perp}_{iz}\rangle = \frac{1}{N}\sum_{k}\left(\langle c^{\dagger}_{ktz\uparrow}c_{kbz\uparrow}\rangle + \langle c^{\dagger}_{-ktz\downarrow}c_{-kbz\downarrow}\rangle\right), \\
&\langle\Delta^{\boldsymbol{x}}_{\mu x}\rangle^{*} = \frac{1}{2N}\sum_{\langle i,j\rangle}\langle\Delta_{ij,\mu x}\rangle^{*} = \frac{1}{N}\sum_{k}2\cos(k_x)\langle c^{\dagger}_{k\mu x\uparrow}c^{\dagger}_{-k\mu x\downarrow}\rangle, \\
&\langle\Delta^{\perp}_{\alpha}\rangle^{*} = \frac{1}{N}\sum_{i}\langle\Delta^{\perp}_{i\alpha}\rangle^{*} = \frac{2}{N}\sum_{k}\langle c^{\dagger}_{kt\alpha\uparrow}c^{\dagger}_{-kb\alpha\downarrow}\rangle
\end{aligned} \tag{S13}
$$

In the two-orbital model, the pairing gap amplitude $\tilde{\Delta}$ is defined as the maximal value of the pairing gap of the $d_{x^2-y^2}$ electrons. For the interlayer s-wave pairing, $\tilde{\Delta}_x = -\frac{3}{8}\tilde{J}_{\perp}\langle\Delta^{\perp}_x\rangle$. For the (s($d_{z^2}$)+id($d_{x^2-y^2}$))-wave pairing, $\tilde{\Delta}_x = -\frac{3}{2}J_{\parallel}\langle\Delta^{\boldsymbol{x}}_{bx}\rangle$.
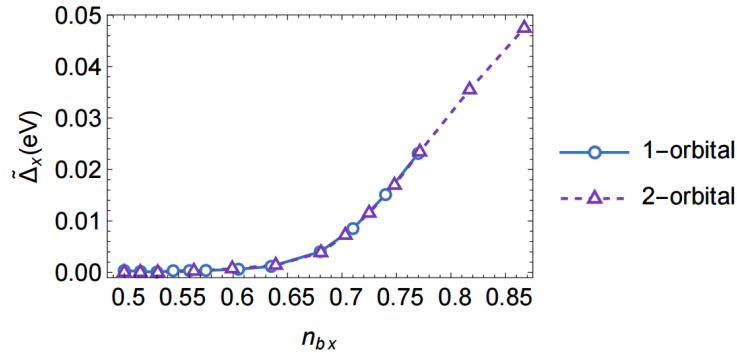

FIG. A3. The comparison of the pairing amplitude $\tilde{\Delta}_x$ as function of the bottom-layer particle number n_{bx} calculated with different models. The lines almost coincide with each other, particularly in the large-n_{bx} regime.

We find that the pairing amplitude $\tilde{\Delta}_x$ as function of the bottom-layer particle number n_{bx} calculated with different models show a strong resemblance (see Fig. A3).

* These two authors contributed equally to this work.
† yangfan_blg@bit.edu.cn

[1] H. Sun, M. Huo, X. Hu, J. Li, Z. Liu, Y. Han, L. Tang, Z. Mao, P. Yang, B. Wang, J. Cheng, D.-X. Yao, G.-M. Zhang, and M. Wang, Nature **621**, 493 (2023).
[2] Y. Zhang, D. Su, Y. Huang, Z. Shan, H. Sun, M. Huo, K. Ye, J. Zhang, Z. Yang, Y. Xu, Y. Su, R. Li, M. Smidman, M. Wang, L. Jiao, and H. Yuan, Nat. Phys. **20**, 1269 (2024).
[3] J. Hou, P.-T. Yang, Z.-Y. Liu, J.-Y. Li, P.-F. Shan, L. Ma, G. Wang, N.-N. Wang, H.-Z. Guo, J.-P. Sun, Y. Uwatoko, M. Wang, G.-M. Zhang, B.-S. Wang, and J.-G. Cheng, Chin. Phys. Lett. **40**, 117302 (2023).
[4] G. Wang, N. N. Wang, X. L. Shen, J. Hou, L. Ma, L. F. Shi, Z. A. Ren, Y. D. Gu, H. M. Ma, P. T. Yang, Z. Y. Liu, H. Z. Guo, J. P. Sun, G. M. Zhang, S. Calder, J.-Q. Yan, B. S. Wang, Y. Uwatoko, and J.-G. Cheng, Phys. Rev. X **14**, 011040 (2024).
[5] G. Wang, N. Wang, Y. Wang, L. Shi, X. Shen, J. Hou, H. Ma, P. Yang, Z. Liu, H. Zhang, X. Dong, J. Sun, B. Wang, K. Jiang, J. Hu, Y. Uwatoko, and J. Cheng, arXiv:2311.08212 (2023).
[6] M. Zhang, C. Pei, Q. Wang, Y. Zhao, C. Li, W. Cao, S. Zhu, J. Wu, and Y. Qi, J. Mater. Sci. Technol. **185**, 147 (2024).
[7] Y. Zhou, J. Guo, S. Cai, H. Sun, P. Wang, J. Zhao, J. Han, X. Chen, Q. Wu, Y. Ding, M. Wang, T. Xiang, H. kwang Mao, and L. Sun, arXiv:2311.12361 (2023).
[8] N. Wang, G. Wang, X. Shen, J. Hou, J. Luo, X. Ma, H. Yang, L. Shi, J. Dou, J. Feng, J. Yang, Y. Shi, Z. Ren, H. Ma, P. Yang, Z. Liu, Y. Liu, H. Zhang, X. Dong, Y. Wang, K. Jiang, J. Hu, S. Calder, J. Yan, J. Sun, B. Wang, R. Zhou, Y. Uwatoko, and J. Cheng, Nature **634**, 579 (2024).
[9] J. Li, P. Ma, H. Zhang, X. Huang, C. Huang, M. Huo, D. Hu, Z. Dong, C. He, J. Liao, X. Chen, T. Xie, H. Sun, and M. Wang, arXiv:2404.11369 (2024).
[10] T. Fukamachi, Y. Kobayashi, T. Miyashita, and M. Sato, J. Phys. Chem. Solids **62**, 195 (2001).
[11] R. Khasanov, T. J. Hicken, D. J. Gawryluk, L. P. Sorel, S. Bötzel, F. Lechermann, I. M. Eremin, H. Luetkens, and Z. Guguchia, arXiv:2402.10485 (2024).
[12] K. Chen, X. Liu, J. Jiao, M. Zou, C. Jiang, X. Li, Y. Luo, Q. Wu, N. Zhang, Y. Guo, *et al.*, Phys. Rev. Lett. **132**, 256503 (2024).
[13] Z. Dan, Y. Zhou, M. Huo, Y. Wang, L. Nie, M. Wang, T. Wu, and X. Chen, arXiv:2402.03952 (2024).
[14] X. Chen, J. Choi, Z. Jiang, J. Mei, K. Jiang, J. Li, S. Agrestini, M. Garcia-Fernandez, X. Huang, H. Sun, D. Shen, M. Wang, J. Hu, Y. Lu, K.-J. Zhou, and D. Feng, arXiv:2401.12657 (2024).
[15] Z. Liu, H. Sun, M. Huo, X. Ma, Y. Ji, E. Yi, L. Li, H. Liu, J. Yu, Z. Zhang, Z. Chen, F. Liang, H. Dong, H. Guo, D. Zhong, B. Shen, S. Li, and M. Wang, Sci. China-Phys. Mech. Astron. **66**, 217411 (2023).
[16] M. Kakoi, T. Oi, Y. Ohshita, M. Yashima, K. Kuroki, T. Kato, H. Takahashi, S. Ishiwata, Y. Adachi, N. Hatada, T. Uda, and H. Mukuda, J. Phys. Soc. Jpn. **93**, 053702 (2024).
[17] T. Xie, M. Huo, X. Ni, F. Shen, X. Huang, H. Sun, H. C. Walker, D. Adroja, D. Yu, B. Shen, L. He, K. Cao, and M. Wang, Sci. Bull. **69**, 3221 (2024).
[18] N. K. Gupta, R. Gong, Y. Wu, M. Kang, C. T. Parzyck, B. Z. Gregory, N. Costa, R. Sutarto, S. Sarker, A. Singer, D. G. Schlom, K. M. Shen, and D. G. Hawthorn, arXiv:2409.03210 (2024).
[19] J.-J. Feng, T. Han, J.-P. Song, M.-S. Long, X.-Y. Hou, C.-J. Zhang, Q.-G. Mu, and L. Shan, Phys. Rev. B **110**, L100507 (2024).
[20] Y. Meng, Y. Yang, H. Sun, S. Zhang, J. Luo, M. Wang, F. Hong, X. Wang, and X. Yu, arXiv:2404.19678 (2024).
[21] S. Fan, Z. Luo, M. Huo, Z. Wang, H. Li, H. Yang, M. Wang, D.-X. Yao, and H.-H. Wen, Phys. Rev. B **110**, 134520 (2024).
[22] M. Xu, G. C. Jose, A. Rutherford, H. Wang, S. Zhang, R. J. Cava, H. Zhou, W. Bi, and W. Xie, arXiv:2410.18840 (2024).
[23] Y. Li, Y. Cao, L. Liu, P. Peng, H. Lin, C. Pei, M. Zhang, H. Wu, X. Du, W. Zhao, K. Zhai, X. Zhang, J. Zhao, M. Lin, P. Tan, Y. Qi, G. Li, H. Guo, L. Yang, and L. Yang, Sci. Bull. (2024), https://doi.org/10.1016/j.scib.2024.10.011.
[24] Z. Liu, M. Huo, J. Li, Q. Li, Y. Liu, Y. Dai, X. Zhou, J. Hao, Y. Lu, M. Wang, and H.-H. Wen, Nat. Commun. **15**, 7570 (2024).
[25] Y. Zhu, D. Peng, E. Zhang, B. Pan, X. Chen, L. Chen, H. Ren, F. Liu, Y. Hao, N. Li, *et al.*, Nature **631**, 531 (2024).
[26] M. Zhang, C. Pei, X. Du, Y. Cao, Q. Wang, J. Wu, Y. Li, Y. Zhao, C. Li, W. Cao, *et al.*, arXiv:2311.07423 (2023).
[27] X. Huang, H. Zhang, J. Li, M. Huo, J. Chen, Z. Qiu, P. Ma, C. Huang, H. Sun, and M. Wang, arXiv:2410.07861 (2024).
[28] Q. Li, Y.-J. Zhang, Z.-N. Xiang, Y. Zhang, X. Zhu, and H.-H. Wen, Chin. Phys. Lett. **41**, 017401 (2024).
[29] J. Zhang, D. Phelan, A. Botana, Y.-S. Chen, H. Zheng, M. Krogstad, S. G. Wang, Y. Qiu, J. Rodriguez-Rivera, R. Osborn, *et al.*, Nat. Commun. **11**, 6003 (2020).
[30] S. Xu, C.-Q. Chen, M. Huo, D. Hu, H. Wang, Q. Wu, R. Li, D. Wu, M. Wang, D.-X. Yao, *et al.*, arXiv:2405.19161 (2024).
[31] X. Du, Y. Li, Y. Cao, C. Pei, M. Zhang, W. Zhao, K. Zhai, R. Xu, Z. Liu, Z. Li, *et al.*, arXiv:2405.19853 (2024).
[32] D. Li, K. Lee, B. Y. Wang, M. Osada, S. Crossley, H. R. Lee, Y. Cui, Y. Hikita, and H. Y. Hwang, Nature **572**, 624

(2019).

[33] K. Lee, B. Y. Wang, M. Osada, B. H. Goodge, T. C. Wang, Y. Lee, S. Harvey, W. J. Kim, Y. Yu, C. Murthy, *et al.*, Nature **619**, 288 (2023).

[34] Y. Nomura and R. Arita, Rep. Prog. Phys. **85**, 052501 (2022).

[35] Q. Gu and H.-H. Wen, The Innovation **3** (2022).

[36] J. Yang, H. Sun, X. Hu, Y. Xie, T. Miao, H. Luo, H. Chen, B. Liang, W. Zhu, G. Qu, *et al.*, Nat. Commun. **15**, 4373 (2024).

[37] L. Wang, Y. Li, S. Xie, F. Liu, H. Sun, C. Huang, Y. Gao, T. Nakagawa, B. Fu, B. Dong, Z. Cao, R. Yu, S. I. Kawaguchi, H. Kadobayashi, M. Wang, C. Jin, H. kwang Mao, and H. Liu, arXiv:2311.09186 (2023).

[38] T. Cui, S. Choi, T. Lin, C. Liu, G. Wang, N. Wang, S. Chen, H. Hong, D. Rong, Q. Wang, Q. Jin, J.-O. Wang, L. Gu, C. Ge, C. Wang, J. G. Cheng, Q. Zhang, L. Si, K. juan Jin, and E.-J. Guo, arXiv:2311.13228 (2023).

[39] X. Sui, X. Han, X. Chen, L. Qiao, X. Shao, and B. Huang, arXiv:2312.01271 (2023).

[40] Z. Luo, X. Hu, M. Wang, W. Wú, and D.-X. Yao, Phys. Rev. Lett. **131**, 126001 (2023).

[41] Y. Zhang, L.-F. Lin, A. Moreo, and E. Dagotto, Phys. Rev. B **108**, L180510 (2023).

[42] Y. Cao and Y.-f. Yang, Phys. Rev. B **109**, L081105 (2024).

[43] Y. Zhang, L.-F. Lin, A. Moreo, T. A. Maier, and E. Dagotto, Nat. Commun. **15**, 2470 (2024).

[44] J. Huang, Z. D. Wang, and T. Zhou, Phys. Rev. B **108**, 174501 (2023).

[45] B. Geisler, J. J. Hamlin, G. R. Stewart, R. G. Hennig, and P. Hirschfeld, npj Quantum Materials **9**, 38 (2024).

[46] L. C. Rhodes and P. Wahl, Phys. Rev. Mater. **8**, 044801 (2024).

[47] Y. Zhang, L.-F. Lin, A. Moreo, T. A. Maier, and E. Dagotto, Phys. Rev. B **109**, 045151 (2024).

[48] N. Yuan, A. Elghandour, J. Arneth, K. Dey, and R. Klingeler, J. Cryst. Growth **627**, 127511 (2024).

[49] J. Li, C.-Q. Chen, C. Huang, Y. Han, M. Huo, X. Huang, P. Ma, Z. Qiu, J. Chen, X. Hu, L. Chen, T. Xie, B. Shen, H. Sun, D. Yao, and M. Wang, Sci. China Phys. Mech. Astron. **67**, 117403 (2024).

[50] B. Geisler, L. Fanfarillo, J. J. Hamlin, G. R. Stewart, R. G. Hennig, and P. Hirschfeld, arXiv:2401.04258 (2024).

[51] H. Li, X. Zhou, T. Nummy, J. Zhang, V. Pardo, W. E. Pickett, J. F. Mitchell, and D. S. Dessau, Nat. Commun. **8**, 704 (2017).

[52] J.-X. Wang, Z. Ouyang, R.-Q. He, and Z.-Y. Lu, Phys. Rev. B **109**, 165140 (2024).

[53] Y. Li, X. Du, Y. Cao, C. Pei, M. Zhang, W. Zhao, K. Zhai, R. Xu, Z. Liu, Z. Li, J. Zhao, G. Li, Y. Qi, H. Guo, Y. Chen, and L. Yang, Chin. Phys. Lett. **41**, 087402 (2024).

[54] M. Li, Y. Wang, C. Pei, M. Zhang, N. Li, J. Guan, M. Amboage, N.-D. Adama, Q. Kong, Y. Qi, and W. Yang, arXiv:2410.04230 (2024).

[55] X. Zhou, W. He, Z. Zhou, K. Ni, M. Huo, D. Hu, Y. Zhu, E. Zhang, Z. Jiang, S. Zhang, S. Su, J. Jiang, Y. Yan, Y. Wang, D. Shen, X. Liu, J. Zhao, M. Wang, M. Liu, Z. Du, and D. Feng, arXiv:2410.06602 (2024).

[56] G. Wang, N. Wang, T. Lu, S. Calder, J. Yan, L. Shi, J. Hou, L. Ma, L. Zhang, J. Sun, B. Wang, S. Meng, M. Liu, and J. Cheng, arXiv:2408.09421 (2024).

[57] C.-Q. Chen, Z. Luo, M. Wang, W. Wú, and D.-X. Yao, Phys. Rev. B **110**, 014503 (2024).

[58] X. Chen, J. Zhang, A. S. Thind, S. Sharma, H. LaBollita, G. Peterson, H. Zheng, D. P. Phelan, A. S. Botana, R. F. Klie, and J. F. Mitchell, J. Am. Chem. Soc. **146**, 3640 (2024).

[59] Z. Dong, M. Huo, J. Li, J. Li, P. Li, H. Sun, L. Gu, Y. Lu, M. Wang, Y. Wang, and Z. Chen, Nature **630**, 847 (2024).

[60] F. Li, N. Guo, Q. Zheng, Y. Shen, S. Wang, Q. Cui, C. Liu, S. Wang, X. Tao, G.-M. Zhang, and J. Zhang, Phys. Rev. Mater. **8**, 053401 (2024).

[61] P. Puphal, P. Reiss, N. Enderlein, Y.-M. Wu, G. Khaliullin, V. Sundaramurthy, T. Priessnitz, M. Knauft, A. Suthar, L. Richter, M. Isobe, P. A. van Aken, H. Takagi, B. Keimer, Y. E. Suyolcu, B. Wehinger, P. Hansmann, and M. Hepting, Phys. Rev. Lett. **133**, 146002 (2024).

[62] Y. Shen, M. Qin, and G.-M. Zhang, Chin. Phys. Lett. **40**, 127401 (2023).

[63] V. Christiansson, F. Petocchi, and P. Werner, Phys. Rev. Lett. **131**, 206501 (2023).

[64] D. A. Shilenko and I. V. Leonov, Phys. Rev. B **108**, 125105 (2023).

[65] W. Wú, Z. Luo, D.-X. Yao, and M. Wang, Sci. China-Phys. Mech. Astron. **67**, 117402 (2024).

[66] X. Chen, P. Jiang, J. Li, Z. Zhong, and Y. Lu, arXiv:2307.07154 (2023).

[67] Z. Ouyang, J.-M. Wang, J.-X. Wang, R.-Q. He, L. Huang, and Z.-Y. Lu, Phys. Rev. B **109**, 115114 (2024).

[68] G. Heier, K. Park, and S. Y. Savrasov, Phys. Rev. B **109**, 104508 (2024).

[69] Y. Wang, K. Jiang, Z. Wang, F.-C. Zhang, and J. Hu, arXiv:2401.15097 (2024).

[70] S. Bötzel, F. Lechermann, J. Gondolf, and I. M. Eremin, Phys. Rev. B **109**, L180502 (2024).

[71] Q.-G. Yang, D. Wang, and Q.-H. Wang, Phys. Rev. B **108**, L140505 (2023).

[72] Y.-B. Liu, J.-W. Mei, F. Ye, W.-Q. Chen, and F. Yang, Phys. Rev. Lett. **131**, 236002 (2023).

[73] F. Lechermann, J. Gondolf, S. Bötzel, and I. M. Eremin, Phys. Rev. B **108**, L201121 (2023).

[74] H. Sakakibara, N. Kitamine, M. Ochi, and K. Kuroki, Phys. Rev. Lett. **132**, 106002 (2024).

[75] Y. Gu, C. Le, Z. Yang, X. Wu, and J. Hu, arXiv:2306.07275 (2023).

[76] C. Lu, Z. Pan, F. Yang, and C. Wu, Phys. Rev. Lett. **132**, 146002 (2024).

[77] H. Oh and Y.-H. Zhang, Phys. Rev. B **108**, 174511 (2023).

[78] Z. Liao, L. Chen, G. Duan, Y. Wang, C. Liu, R. Yu, and Q. Si, Phys. Rev. B **108**, 214522 (2023).

[79] X.-Z. Qu, D.-W. Qu, J. Chen, C. Wu, F. Yang, W. Li, and G. Su, Phys. Rev. Lett. **132**, 036502 (2024).

[80] Y.-F. Yang, G.-M. Zhang, and F.-C. Zhang, Phys. Rev. B **108**, L201108 (2023).

[81] K. Jiang, Z. Wang, and F.-C. Zhang, Chin. Phys. Lett. (2023).

[82] Y. Zhang, L.-F. Lin, A. Moreo, T. A. Maier, and E. Dagotto, Phys. Rev. B **108**, 165141 (2023).
[83] Q. Qin and Y.-F. Yang, Phys. Rev. B **108**, L140504 (2023).
[84] Y.-H. Tian, Y. Chen, J.-M. Wang, R.-Q. He, and Z.-Y. Lu, Phys. Rev. B **109**, 165154 (2024).
[85] R. Jiang, J. Hou, Z. Fan, Z.-J. Lang, and W. Ku, Phys. Rev. Lett. **132**, 126503 (2024).
[86] D.-C. Lu, M. Li, Z.-Y. Zeng, W. Hou, J. Wang, F. Yang, and Y.-Z. You, arXiv:2308.11195 (2023).
[87] N. Kitamine, M. Ochi, and K. Kuroki, arXiv:2308.12750 (2023).
[88] Z. Luo, B. Lv, M. Wang, W. Wú, and D.-X. Yao, npj Quantum Materials **9**, 61 (2024).
[89] J.-X. Zhang, H.-K. Zhang, Y.-Z. You, and Z.-Y. Weng, Phys. Rev. Lett. **133**, 126501 (2024).
[90] Z. Pan, C. Lu, F. Yang, and C. Wu, arXiv:2309.06173 (2023).
[91] H. Sakakibara, M. Ochi, H. Nagata, Y. Ueki, H. Sakurai, R. Matsumoto, K. Terashima, K. Hirose, H. Ohta, M. Kato, Y. Takano, and K. Kuroki, Phys. Rev. B **109**, 144511 (2024).
[92] H. Lange, L. Homeier, E. Demler, U. Schollwöck, A. Bohrdt, and F. Grusdt, Phys. Rev. B **110**, L081113 (2024).
[93] H. Yang, H. Oh, and Y.-H. Zhang, arXiv:2309.15095 (2023).
[94] H. Lange, L. Homeier, E. Demler, U. Schollwöck, F. Grusdt, and A. Bohrdt, arXiv:2309.15843 (2023).
[95] T. Kaneko, H. Sakakibara, M. Ochi, and K. Kuroki, Phys. Rev. B **109**, 045154 (2024).
[96] Z. Fan, J.-F. Zhang, B. Zhan, D. Lv, X.-Y. Jiang, B. Normand, and T. Xiang, Phys. Rev. B **110**, 024514 (2024).
[97] X. Wu, H. Yang, and Y.-H. Zhang, Phys. Rev. B **110**, 125122 (2024).
[98] Y. Zhang, L.-F. Lin, A. Moreo, T. A. Maier, and E. Dagotto, Phys. Rev. Lett. **133**, 136001 (2024).
[99] M. Zhang, H. Sun, Y.-B. Liu, Q. Liu, W.-Q. Chen, and F. Yang, Phys. Rev. B **110**, L180501 (2024).
[100] Q.-G. Yang, K.-Y. Jiang, D. Wang, H.-Y. Lu, and Q.-H. Wang, Phys. Rev. B **109**, L220506 (2024).
[101] Y. Zhang, L.-F. Lin, A. Moreo, T. A. Maier, and E. Dagotto, Phys. Rev. B **110**, L060510 (2024).
[102] Y.-F. Yang, Phys. Rev. B **110**, 104507 (2024).
[103] S. Ryee, N. Witt, and T. O. Wehling, Phys. Rev. Lett. **133**, 096002 (2024).
[104] C. Lu, Z. Pan, F. Yang, and C. Wu, Phys. Rev. B **110**, 094509 (2024).
[105] Z. Ouyang, M. Gao, and Z.-Y. Lu, npj Quantum Materials **9**, 80 (2024).
[106] H. LaBollita, V. Pardo, M. R. Norman, and A. S. Botana, arXiv:2309.17279 (2024).
[107] B. Zhang, C. Xu, and H. Xiang, arXiv:2407.18473 (2024).
[108] I. V. Leonov, arXiv:2410.15298 (2024).
[109] H. LaBollita, V. Pardo, M. R. Norman, and A. S. Botana, arXiv:2407.14409 (2024).
[110] X.-S. Ni, Y. Ji, L. He, T. Xie, D.-X. Yao, M. Wang, and K. Cao, arXiv:2407.19213 (2024).
[111] X.-W. Yi, Y. Meng, J.-W. Li, Z.-W. Liao, W. Li, J.-Y. You, B. Gu, and G. Su, Phys. Rev. B **110**, L140508 (2024).
[112] H. LaBollita, J. Kapeghian, M. R. Norman, and A. S. Botana, Phys. Rev. B **109**, 195151 (2024).
[113] K.-Y. Jiang, Y.-H. Cao, Q.-G. Yang, H.-Y. Lu, and Q.-H. Wang, arXiv:2409.17861 (2024).
[114] Y. Chen, Y.-H. Tian, J.-M. Wang, R.-Q. He, and Z.-Y. Lu, arXiv:2407.13737 (2024).
[115] Y. Zhang, L.-F. Lin, A. Moreo, T. A. Maier, and E. Dagotto, arXiv:2408.07690 (2024).
[116] L.-F. Lin, Y. Zhang, N. Kaushal, G. Alvarez, T. A. Maier, A. Moreo, and E. Dagotto, arXiv:2408.05689 (2024).
[117] C. Qin, K. Foyevtsova, L. Si, G. A. Sawatzky, and M. Jiang, arXiv:2410.15649 (2024).
[118] I. V. Leonov, Phys. Rev. B **109**, 235123 (2024).
[119] Y.-B. Liu, H. Sun, M. Zhang, Q. Liu, W.-Q. Chen, and F. Yang, arXiv: (2024).
[120] G. Kotliar and J. Liu, Phys. Rev. B **38**, 5142 (1988).